Missing baryons in the cosmic web revealed by the Sunyaev-Zel'dovich effect

Anna de Graaff[1], Yan-Chuan Cai[1], Catherine Heymans[1] & John A. Peacock[1]

[1]*Institute for Astronomy, University of Edinburgh, Royal Observatory, Blackford Hill, Edinburgh, EH9 3HJ, UK*

arXiv:1709.10378v2 [astro-ph.CO] 5 Oct 2017

Observations of galaxies and galaxy clusters in the local universe can account for only 10% of the baryon content inferred from measurements of the cosmic microwave background and from nuclear reactions in the early Universe[1–3]. Locating the remaining 90% of baryons has been one of the major challenges in modern cosmology. Cosmological simulations predict that the 'missing baryons' are spread throughout filamentary structures in the cosmic web, forming a low density gas with temperatures of $10^5 - 10^7$ K[4,5]. Previous attempts to observe this diffuse warm-hot filamentary gas via X-ray emission or absorption in quasar spectra have been inconclusive[6–9]. Here we report a 5.1σ detection of warm-hot baryons in stacked filaments through the thermal Sunyaev-Zel'dovich (SZ) effect, which arises from the distortion in the cosmic microwave background spectrum due to ionised gas[10]. The estimated gas density in these 15 Megaparsec-long filaments is approximately 6 times the mean universal baryon density, and overall this can account for $\sim 30\%$ of the total baryon content of the Universe. This result establishes the presence of ionised gas in large-scale filaments, and suggests that the missing baryons problem may be resolved via observations of the cosmic web.

The matter distribution of the Universe follows a web-like pattern, generated by the gravitational instability of small initial density fluctuations. Galaxies and galaxy clusters are embedded in the knots of the web (known as dark matter haloes), and are connected by large-scale filamentary and sheet-like structures. Both observations and simulations suggest that a significant fraction of baryons should be found outside the gravitationally bound haloes, in filaments and sheets[4,8,9]. The baryons are expected to be in a diffuse 'warm-hot' state, with a density of the order ten times the mean baryon density and temperatures between $10^5 - 10^7$ K. Previous efforts to detect this warm-hot intergalactic medium focused on the measurement of absorption lines in the spectra of distant quasars[8], and on the X-ray emission from individual cosmic web filaments[6,7]. These methods however probed only the lower and higher temperature end of the warm-hot baryons, leaving the majority of the baryons still unobserved[9].

The thermal Sunyaev-Zel'dovich effect provides an alternative means of detecting the warm-hot baryons in filaments. The SZ effect arises from the Compton scattering of photons from the cosmic microwave background by ionised gas. The amplitude of the signal is quantified by the Compton y-parameter, which is proportional to the line-of-sight integration of the free electron gas pressure (i.e. $y \propto n_{\rm e} T_{\rm e}$, where $n_{\rm e}$ and $T_{\rm e}$ are the density and temperature of free electrons respectively). We search for gas filaments using the all-sky Compton 'y-map' from the Planck collaboration[11], for which the locations and orientations of filaments on the map need to be known.

From analyses of numerical simulations, we expect filaments to connect pairs of massive haloes separated by up to $\sim 20\,h^{-1}$ Mpc [12]. As such, a good proxy for the location of filaments is the line connecting neighbouring massive galaxies. We therefore search for pairs of galaxies in the constant mass (CMASS) galaxy catalogue from the Sloan Digital Sky Survey Data Release 12[13,14]. These galaxies are, on average, hosted by dark matter haloes with a virial mass of $\sim 10^{13}\,h^{-1} M_\odot$, where $M_\odot$ is the mass of the Sun and h is the dimensionless Hubble parameter.

For this analysis, we consider galaxy pairs that are well separated, to minimise the contamination to the filament signal by the two host haloes. We select pairs with a projected separation on

the sky of $6 - 14\,h^{-1}$ Mpc and a line-of-sight separation $< 5\,h^{-1}$ Mpc [15], finding one million pairs of galaxies with a mean pair separation of $\sim 10\,h^{-1}$ Mpc. This is well beyond the virial radius of their host dark matter haloes, which is on average less than $1\,h^{-1}$ Mpc.

To stack the SZ signal with the galaxy pairs, we rotate and rescale the y-map for each pair according to their location, orientation and separation distance such that the positions of all pairs of galaxies overlap on the stacked y-map. The resulting stacked y-map from the 1 million pairs is presented in the left panel of Fig. 1. The map is dominated by the SZ signal from the two bright galaxy haloes. The main important feature however, is the bridge connecting the two haloes, which suggests the presence of a filament.

We search for an SZ signal from the filament by removing the isotropic contribution from the two haloes. To determine this contribution, we use the mean radial profile of the halo extracted from 60-degree sectors perpendicular to the pair separation ($r_\perp$ in Fig. 1; see Methods). This profile is chosen to exclude any signal from a filament, which lies along the horizontal direction ($r_\parallel$). However, the contribution from the secondary halo may still be non-negligible. Assuming spherical symmetry, we then decompose the mean radial profile to account for both haloes and fit their individual contributions. The profile is shown in the upper left panel of Fig. 2 together with the components of the best-fit model: the primary halo (blue, dashed line), secondary halo (green, dash-dotted line) and combined contributions (pink, solid line). The residuals between the profile and modelled contribution from the two haloes (lower left panel of Fig. 2) are small, indicating the accuracy of the modelling. The constructed 2-dimensional best-fit model for the SZ signal from the two haloes (without any filament) is shown in the middle panel of Fig. 1. The difference between this model and the stacked data (left) is shown on the right. No significant residual of the two main haloes is found, with the exception of the region interior to the halo centres (indicated by the dashed box), as is expected if there is an SZ signal associated with filaments. The extracted 1-dimensional horizontal profiles for the stacked data and model are presented in the upper right panel of Fig. 2. The corresponding 1-dimensional residual signal is shown in the lower right panel. We find the excess signal seen in between the halo centres (indicated by dotted lines) to be significant at the

5.1σ level. There is also noticeable excess signal in the outer region of the galaxy pairs, which plausibly arises from filaments extending beyond the pair. By taking into account both the inner and outer regions, we detect the filament at the 3.8σ level.

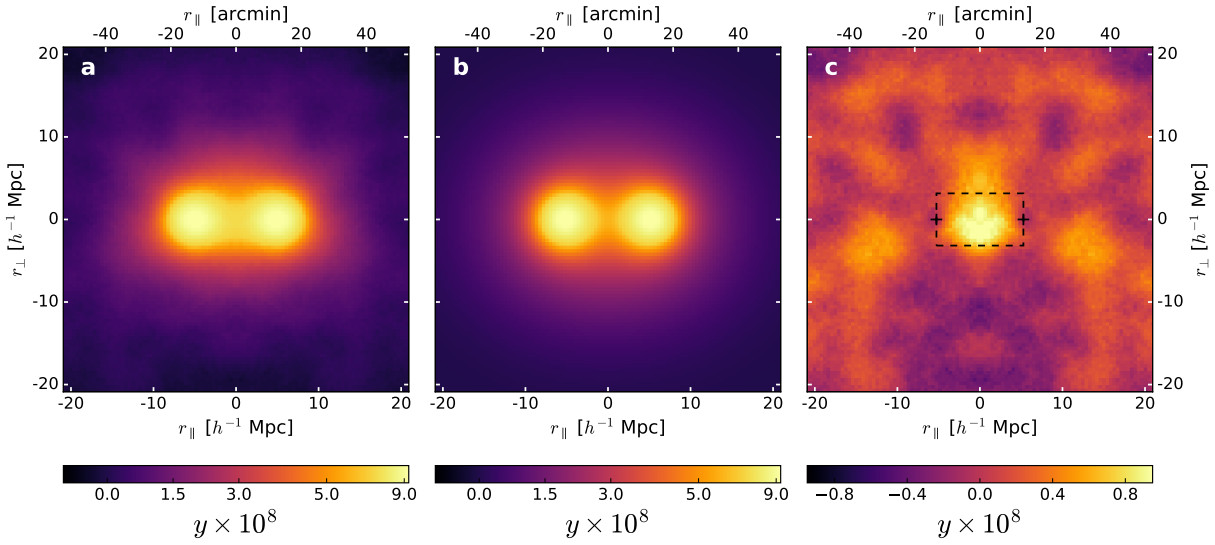

Figure 1: The SZ effect for 1 million stacked pairs of galaxies. (a) the symmetrically stacked Compton y-parameter maps for 1 million close pairs of CMASS galaxies; (b) the modelled signal from the galaxy host haloes only; and (c) the residual between the stacked data and model. The colour bar indicates the magnitude of the SZ effect through the dimensionless y-parameter, which is related to the pressure of the ionised gas. The indicated horizontal and vertical distance scales ($r_\parallel$ and $r_\perp$ respectively) are calibrated using the mean galaxy pair separation of $10.5\,h^{-1}$ Mpc. The mean projected angular separations are also shown for the horizontal axis. There is a bridge connecting the pairs of galaxies in the data (a) but not in the model (b), which indicates the presence of a filament in (a). The detected filament is highlighted in panel (c) by a dashed box with plus signs indicating the positions of the galaxy pairs.

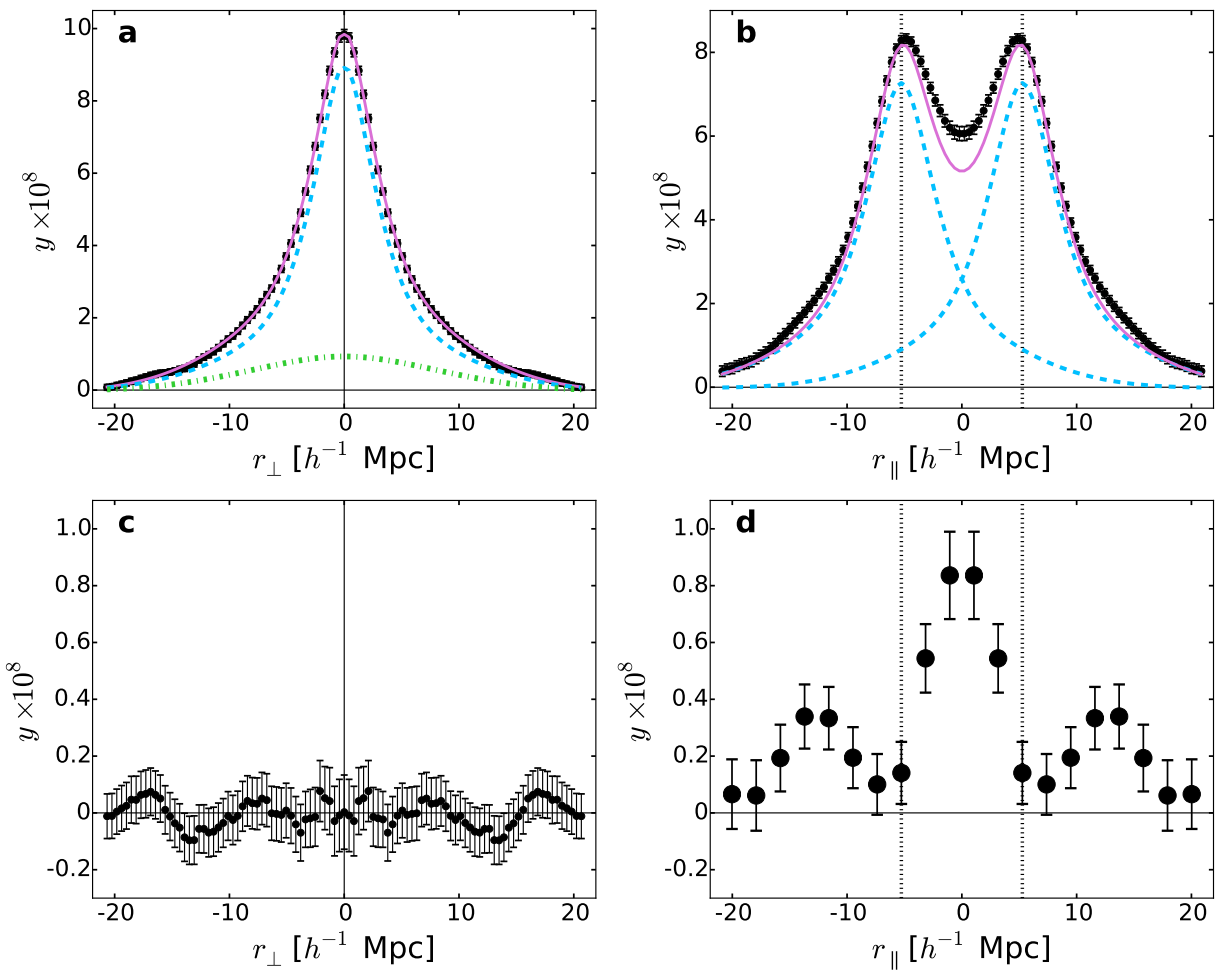

Figure 2: 1-dimensional profiles of the SZ signal from stacked galaxy pairs. (a) The mean radial SZ profile extracted along the vertical direction in the left-hand panel of Fig. 1; (b) the mean horizontal profile with a thickness of 6 h^{-1}Mpc extracted from the left-hand panel of Fig. 1; the residual of (c) the radial profile and (d) the horizontal profile after subtracting the contribution from the two haloes. Error bars represent statistical uncertainties obtained from the individual profiles. The blue dashed lines and the green dash-dotted line indicate the modelled primary and secondary halo contributions respectively. The pink solid lines show the combined modelled contribution from the two haloes. The residual in (c) is consistent with zero, indicating the success of our modelling. The detected filament lies interior to the halo centres (dotted lines), shown by the offset between the solid pink line and the black data points in (b), and by the residuals in (d).

If we accept the reality of the filament signal, there remains the question of whether the effect arises from diffuse gas, or from gas within galaxy haloes that are part of the large-scale structure around the target halo pairs. We distinguish between uncorrelated structures, which lie projected along the line of sight to the galaxy pairs, and structures that are correlated with the galaxy pairs. We estimate the residual SZ signal due to the uncorrelated large-scale structures by repeating our stacking and fitting procedure for a second class of galaxy pairs known as 'non-physical pairs'[16] (see Methods). These galaxy pairs are selected to have the same projected distance separations as the primary sample of physical pairs, but with much larger line-of-sight separations, such that they are unlikely to be connected by filaments. The residual SZ signal between the non-physical pairs is consistent with zero, contributing at most $\sim 10\%$ of the filament signal between the physical pairs. We next estimate the contribution of correlated large-scale structures by repeating our analysis for an all-sky map of the projected number density of CMASS galaxies. We estimate that gas in these galaxies will contribute $\sim 10\%$ of the detected filament SZ signal (see Methods). Therefore, in total at most $\sim 20\%$ of the filament SZ signal could be contributed by the alignment of galaxies or groups of galaxies along the line of sight to the filament.

The amplitude of the filament signal has a maximum value of $y = 9 \times 10^{-9}$ for the gas pressure parameter y, and peaks half way between the two haloes. The signal is therefore unlikely to be contaminated by either of the two haloes (see Methods). Cosmological hydrodynamical simulations suggest that the gas in filaments is most likely to be at a temperature of 10^6 K[4,5,9]. Assuming this gas temperature, we estimate the filament gas density to be approximately six times the mean baryon density of the Universe. This is consistent with expectations from simulations. Accounting for the entire volume of the CMASS galaxy sample, the ionised gas in these filaments accounts for approximately 30% of the total baryon content of the Universe.

This is the baryon fraction found in filaments derived from our specific selection in terms of filament length and galaxy pair population, so it is certainly incomplete. We expect that more gas in filaments can be detected using deeper galaxy surveys, in which smaller filaments will be found. Moreover, the gas density of these filaments detected via the SZ effect can be determined

more accurately if there are other means of observational constraints for the gas temperature. For example, a high resolution soft X-ray survey will be ideal to help break the degeneracy between gas temperature and density. Nevertheless, our finding provides strong evidence for the presence of warm-hot gas in filaments and opens up a new window to search for missing baryons in the cosmic web.

Methods

Selection of galaxy pairs. We use both the North and South CMASS galaxy catalogues from the 12$^{\text{th}}$ data release of the Sloan Digital Sky Survey (SDSS)[13,14]. The CMASS galaxies were selected using colour-magnitude cuts to identify galaxies in the redshift range $0.43 < z < 0.75$ with a narrow range in stellar mass. The galaxies have a mean stellar mass of $10^{11.3} M_{\odot}$ and are mostly central galaxies in their host dark matter haloes of typical virial mass $\sim 10^{13}\, h^{-1}\, M_{\odot}$ [17,18]. CMASS galaxies therefore represent a highly biased galaxy sample.

Using the full CMASS catalogue of 0.85 million galaxies, we select a sample of galaxy pairs that are likely to be connected by filaments ('physical pairs'). Motivated by Clampitt et al.[15], the pairs are required to have a transverse comoving separation in the range $6 - 14\, h^{-1}$ Mpc and a line-of-sight separation $< 5\, h^{-1}$ Mpc. These ranges were chosen to ensure that the intergalactic medium is probed as well as the intracluster medium within the haloes (of virial radius $\sim 1\, h^{-1}$ Mpc). By applying the first constraint we prevent contamination from the potential projection of two haloes along the line of sight. The final selection of physical pairs comprises $1\,020\,334$ pairs with a mean angular separation of 26.5 arcmin and a mean comoving separation of $10.5\, h^{-1}$ Mpc.

In addition to our filament candidates, we compile a second sample of 'non-physical' pairs of galaxies that have the same comoving projected separation of $6 - 14\, h^{-1}$ Mpc, but are separated by $40 - 200\, h^{-1}$ Mpc along the line of sight. These pairs of galaxies therefore appear close in projection, yet are highly unlikely to be connected by filaments[16]. The resulting selection of $13\,622\,456$ non-physical pairs has a distribution of angular separations similar to that of the physical pairs. We use this catalogue to estimate the contribution from uncorrelated large-scale structures to the SZ

signal in the filament region.

Compton parameter map stacking. We use the MILCA (Modified Internal Linear Combination Algorithm)[19] all-sky Compton parameter map ('y-map') released by the Planck Collaboration[11]. This y-map was constructed from the multiple Planck frequency channel maps, which were convolved to a common resolution with a circular Gaussian beam of FWHM $= 10$ arcmin. We apply a 30% Galactic mask provided by the Planck Collaboration to reduce contamination from galactic emission and point sources. Both the y-map and mask are provided in the HEALPix[20] format at a resolution of $N_{\rm side} = 2048$.

As the expected SZ signal from a single filament falls well below the noise level of the y-map, we stack the signal from the full sample of galaxy pairs. The map area surrounding each galaxy pair is rotated such that the galaxy pair aligns with the equator, with the centre of the pair located at the origin of the galactic coordinate system. The rotated areas are then rescaled according to their corresponding angular pair separation, such that the locations of the different pairs overlap with each other. We then project each map onto a 2-dimensional rectangular grid using a nearest neighbour interpolation. For every galaxy pair we stack both the projected map and its mirrored version, thus resulting in a stacked map symmetrical in the vertical axis (see left-hand panel of Fig. 1). Masked HEALPix pixels are accounted for by assigning a weight of zero to the corresponding grid pixels.

In order to improve the computational efficiency of our stacking algorithm, we reduce the map resolution to $N_{\rm side} = 1024$, corresponding to a typical pixel size of 3.4 arcmin. The y-map is stacked for the physical pairs as well as for 500 subsamples of non-physical pairs, each containing 1.02 million randomly selected pairs.

Modelling the contribution from the two isolated haloes. We model the contribution from the two haloes to the stacked SZ signal (Fig. 1) in order to look for a residual signal. The two-halo contribution is assumed to be the superposition of two isotropic profiles, and approximated with the averaged profile within a 60-degree subtended angle along the vertical direction (as indicated

in Fig. 3). The vertical branch of the profile is used in order to avoid possible contamination from the tentative filament, which is most likely to be along the horizontal direction. We assume the radial y-profile of the halo can be described by some unknown function $f(r)$. Since the stacking procedure is symmetrical about the vertical axis, the two haloes are described by the same function. Along the vertical direction, at a radius r_1 from the halo centre on the left, the SZ signal contains contributions from both haloes. The total SZ signal then is $F(r_1)$, where $F(r_1) = f(r_1) + f(r_2)$ and $r_2 = (r_1^2 + r_{12}^2)^{1/2}$ (see Fig. 3). We use a fourth order polynomial multiplied by an exponential function for $f(r)$, which is found to provide an accurate fit to the data with residuals at the 1×10^{-9} level. From this model we then generate a 2D y-map of the two haloes, and subtract it from the data. The only significant signal in the residual map (right-hand panel of Fig. 1) is found to lie in the region interior to the two haloes.

The filament signal is at most $\sim 10\%$ of the overlapping isotropic signals from the two haloes, so some care is needed in order to be convinced that the residual cannot be an artefact of any error in the assumed halo profiles. In particular, if the true halo profiles were slightly broader than our best-fit model, this would raise the signal in the overlap region between the haloes. To investigate this, we introduced an additional nuisance parameter, in which the true halo profile is expanded in radius by a factor s compared to our estimate. The parameter s was then allowed to float in order to best-fit the full 2D data in Fig. 1, adopting the null hypothesis that no filament is present. We also allowed a free vertical normalization in this exercise. In fact, the preference is for a slightly *narrower* profile, with $s = 0.94$, driven by the negative residuals at large $r_\perp$ and small $r_\parallel$. In any case, this scaling changes the inferred filament signal by only $\sim 10\%$. We therefore conclude that our main result is robust with respect to the assumed model for the isotropic halo profile.

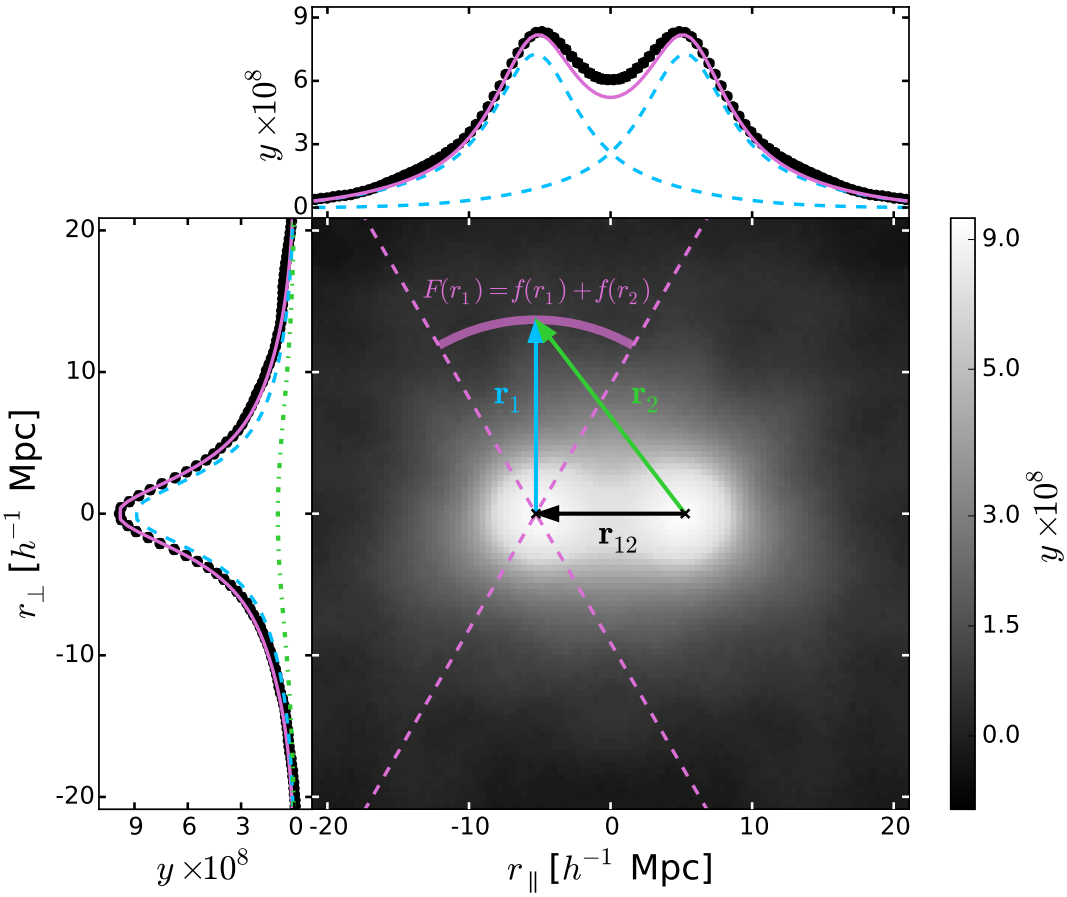

Figure 3: Construction of 1-dimensional profiles. Illustration for the fitting procedure to decompose the contribution from the isotropic haloes and the filament. The stacked CMASS galaxy pairs for the Compton y-map are shown in black and white in the main panel. The mean horizontal profile extracted from the 2D plot is in the upper panel. The pink dashed lines indicate the 60-degree subtended angle used to construct the mean radial profile in the left panel. The arrows demonstrate how the two haloes were decomposed for the halo modelling. Blue colours correspond to the primary halo contribution, green to the secondary halo, and pink to the combined contribution from the two haloes. $F(r)$ indicates the sum of the two isotropic halo profiles [$f(r_1)$ and $f(r_2)$] along the vertical direction. The good agreement between the model and the data points for the vertical profile allows us to estimate the filament signal indicated by the offset between the model and the data points in the upper panel.

Estimating the significance of the filament. To estimate the significance of the tentative filament signal, we measure the profile of the residual y-map along the horizontal direction with a width of $\sim 6\,h^{-1}$ Mpc, as indicated by the right-hand panel in Fig. 1. The width of the filament was chosen to be approximately 1.5×FWHM of the beam profile for the y-map. We construct the covariance of the data points using individual y-maps associated with each pair,

$$C_{i,j} = \frac{1}{N}\sum_{k=1}^{N}(y_i^k - \bar{y_i}^k)(y_j^k - \bar{y_j}^k), \tag{1}$$

where the subscript i and j indicate the indices of the bins, the superscript k represents the index of galaxy pair and $N = 1\,020\,334$ is the total number of pairs. The normalised covariance matrix is shown in Fig. 4. We next compute the total χ^2 value,

$$\chi^2 = \sum_{i,j}^{n} \bar{y_i} C_{i,j}^{-1} \bar{y_j}, \tag{2}$$

where n is the number of bins. The χ^2 values were converted into the corresponding Gaussian σ values taking into account the number of degrees of freedom. The data points between the two galaxies, which we interpret as being due to gas filaments, deviate from the zero point at the 5.1σ confidence level. We also find a lower-significance horizontal excess of the SZ signal outside the galaxy pairs, which may be the extension of the filament. Including these data points in the average decreases the significance of the filament by approximately 1σ.

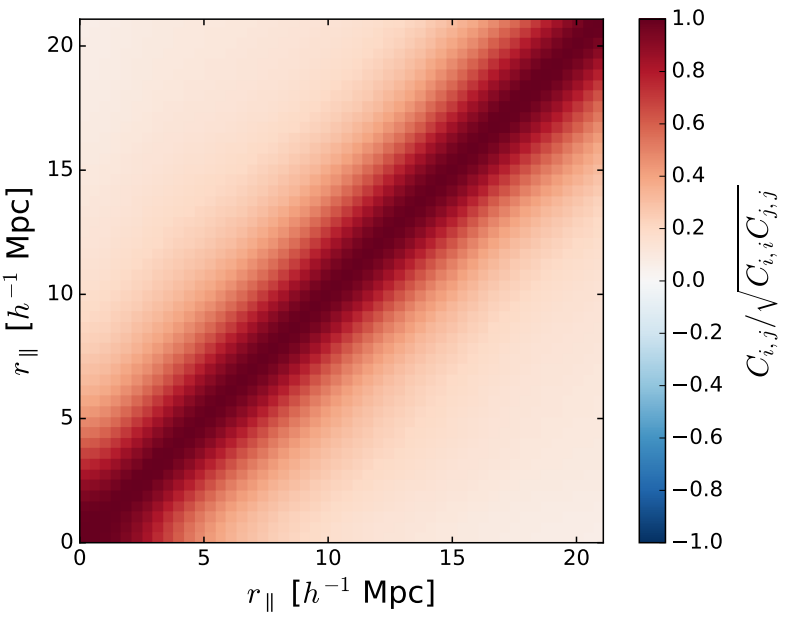

Figure 4: Normalised covariance matrix. The constructed normalised covariance matrix of the data points from the horizontal profile in Fig. 2. Since the two sides of the profile are perfectly symmetric, only one quarter of the matrix is shown. This covariance matrix is used to estimate the statistical significance of the filament signal using Equation 2.

In principle, the excess signal between the two pairs can also be contributed by gas in galaxies that are part of large-scale structures projected along the line of sight. To estimate the contribution of uncorrelated large-scale structures, we repeat our analysis for the catalogue of non-physical galaxy pairs. We use 13.6 million selected non-physical CMASS galaxy pairs to draw 500 subsamples of equal size to the sample of physical pairs, and then perform the stacking, halo modelling and profile extraction for each subsample. The mean residual SZ signal for the non-physical pairs is found to be $y = (6 \pm 3) \times 10^{-10}$ with a significance level of 0.2σ (Fig. 5). We therefore conclude that the uncorrelated large-scale structures cannot make a significant contribution to the SZ signal of the detected filament.

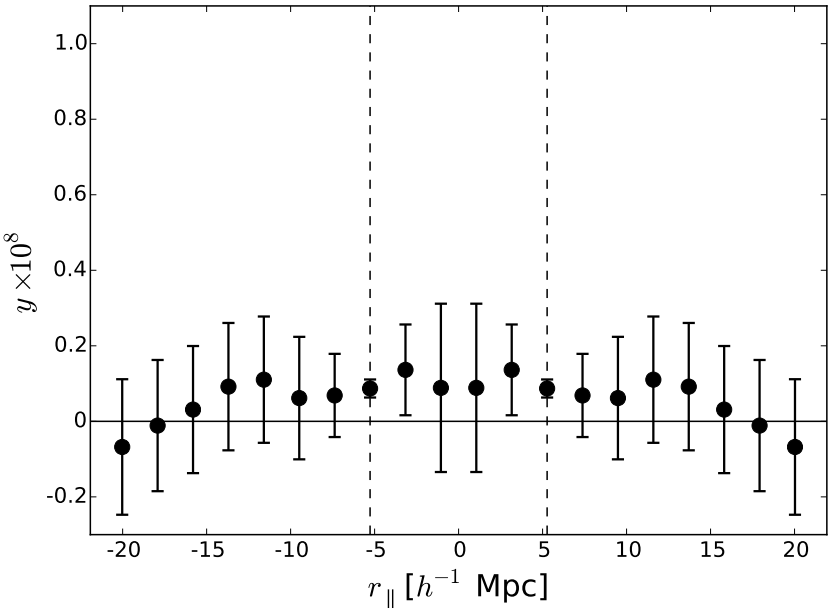

Figure 5: Residual SZ signal of the non-physical pairs. The mean horizontal residual SZ signal of the 500 subsamples of non-physical pairs. Dashed lines indicate the positions of the galaxy pairs. The error bars show statistical uncertainties obtained from the 500 residual profiles. The residuals are consistent with zero within the errors, with $y = (6 \pm 3) \times 10^{-10}$ between the two haloes. This accounts for $\lesssim 10\%$ of the filament signal and is therefore subdominant.

Since the non-physical pairs have larger distance separations than the physical pairs, they may not represent the probability of the alignment of further haloes between the galaxy pairs. We further examine the effect of possible correlated structures, by constructing a map of the galaxy number density for the whole CMASS sample. The map was convolved with a Gaussian filter of FWHM $= 10$ arcmin to represent the beam size of the y-map. We repeat the same stacking and fitting procedure for the physical pairs with the galaxy number density map. The resulting 2D stacked pairs and residual profiles are shown in Fig. 6 together with the extracted profiles and fitted models. After subtraction of the isotropic component of the two haloes, we find that a filament in the light distribution between the galaxy pairs is detected. However, the relative level of this signal is small: 1-2% of the peak values of the two haloes, as against about 10% in the SZ analysis. We therefore estimate that correlated galaxy haloes contribute approximately 10% of the detected filament signal.

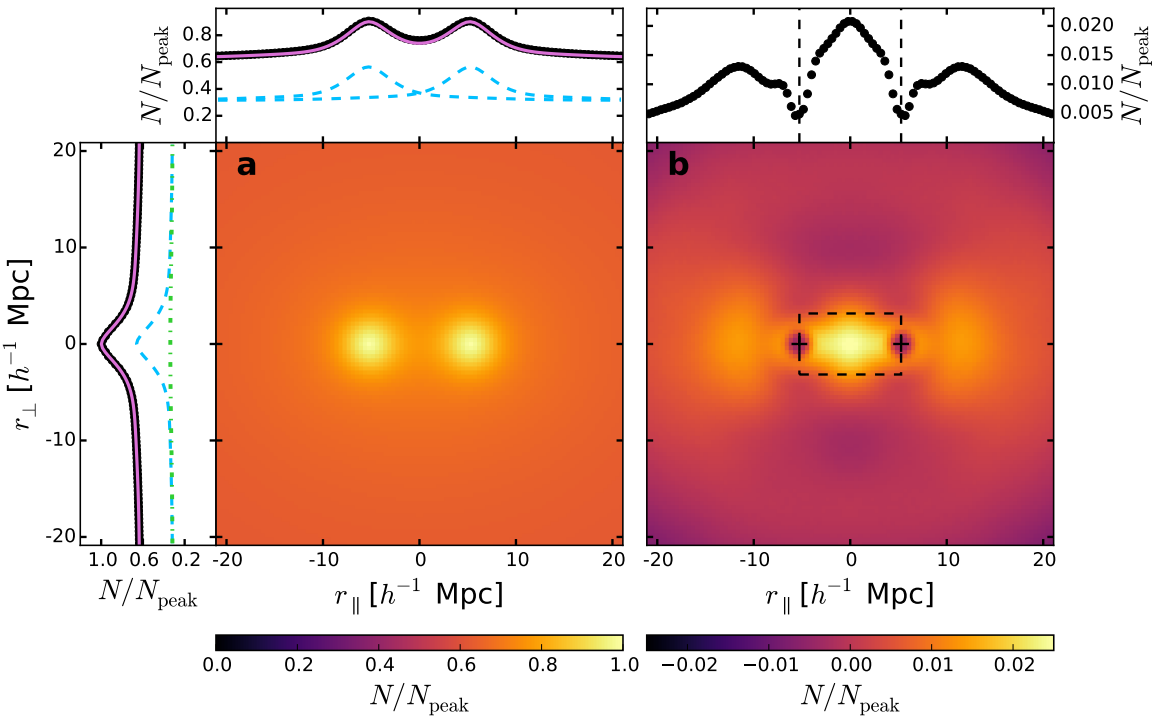

Figure 6: The mean galaxy number density around the galaxy pairs. (a) The main panel shows the stacked CMASS galaxy number density map for 1 million galaxy pairs, convolved with a Gaussian filter with FWHM$=10$ arcmin and normalised by the peak value of the stacked map. The left and upper side-panels show the mean radial profile and horizontal profile respectively, and include the modelled contributions from the primary halo (blue, dashed lines), secondary (green, dash-dotted line) and the two haloes combined (pink, solid lines). (b) The residual between the stacked map and two isotropic halo profiles. The upper side-panel shows the residual profile extracted from the boxed region, with dashed lines indicating the galaxy pair centres. The residual haloes in the filament region are estimated to contribute approximately 10% of the filament signal.

In making the estimate of the contribution to the filament signal from galaxies within the filament, we have to consider also the contribution from galaxies below the CMASS limit. These are significant in principle: taking the relation between the SZ decrement and stellar mass from Greco et al.[21] and the stellar mass function at $z = 0.55$ from Maraston et al.[17], we estimate that galaxies at or above the CMASS stellar mass contribute approximately 1/3 of the global SZ signal.

If the low-mass galaxies clustered about CMASS galaxies in the same way as CMASS galaxies, then their contribution would be correctly included by our analysis. The most extreme alternative would be if low-mass galaxies completely avoided CMASS galaxies within a few Mpc, in which case our CMASS scaling analysis would not include their contribution. The contribution of gas in haloes to the filament would then have to increase by a full factor of 3. There will be some such effect, because the one-halo correlations around CMASS galaxies will only have satellites smaller than around 1/10 the CMASS galaxy mass. However, given the large Planck beam, the main effect in the smoothed maps is most likely dominated by the two-halo effect. We therefore expect any correction from gas in low-mass galaxies to be much less than the global factor 3, noting that even such an extreme correction would not be enough to account for the SZ signal that we have observed.

Estimating the baryon fraction in filaments. The full expression for the SZ Compton y-parameter[10] is

$$y = \int \frac{k_{\rm B} T_{\rm e}}{m_{\rm e} c^2} \, n_{\rm e} \, \sigma_{\rm T} \, {\rm d}\ell, \tag{3}$$

where $m_{\rm e}c^2$, $k_{\rm B}$ and $\sigma_{\rm T}$ are the electron rest mass energy, Boltzmann constant and the Thomson cross-section respectively, all of which are known physical quantities that amount to a constant. The y-parameter therefore depends solely on the line-of-sight integration of $n_{\rm e}T_{\rm e}$, which are respectively the electron gas density and temperature. There is a degeneracy between the gas density and temperature, which can in principle be broken by additional observations for one of the quantities. Previous studies of warm-hot gas filaments using hydrodynamical simulations[4,5] have suggested that the gas in filaments is most likely to have been shock heated to temperatures of approximately 10^6 K. Given the lack of evidence from current X-ray observations for gas filaments at scales of a few h^{-1}Mpc, a higher ($T_{\rm e} > 10^7$ K) gas temperature seems unlikely. We therefore assume the gas temperature to be $T_{\rm e} = 10^6$ K by default.

We further assume that the filament takes the shape of a cylinder in which the gas density follows a 2-dimensional Gaussian profile. Unlike the line-of-sight direction, along the vertical direction ($r_\perp$) the SZ signal and hence the electron number density $n_{\rm e}$ will also be convolved with

the Planck beam of FWHM $= 10$ arcmin. We adopt a FWHM for the intrinsic filament profile of $1.5\,h^{-1}$ Mpc [12]; our result for the total baryon content of the filament is almost independent of this choice, since the large Planck beam is dominant. From our analysis we found the mean amplitude of the filament between the two pairs to be $\bar{y} \approx 0.6 \times 10^{-8}$. Taking $T_{\rm e} = 10^6$ K and using the cylindrical Gaussian model, we determine the central density in the filament to be $n_{\rm e}(z) \approx 6 \times \bar{n}_{\rm e}(z)$, where $\bar{n}_{\rm e}(z)$ is the mean universal electron density at the medium redshift of the CMASS galaxy sample $z = 0.55$. Assuming the universe to be fully ionised and accounting for the full volume covered by the CMASS survey of $\sim 4\,(h^{-1}$ Gpc$)^3$, this estimated filament density amounts to approximately 30% of the mean baryon density of the Universe[3]: $0.3\Omega_{\rm b}$.

Similar conclusions to this work have been independently drawn by Tanimura et al.[22] (hereafter referred to as T17) who announced their analysis of the SZ signal between neighbouring galaxy pairs at the same time as this publication. Our study differs from T17 mainly in the galaxy pair catalogues used: T17 used the SDSS-DR12 LRG galaxy catalogue and found $262\,864$ pairs of galaxies at redshifts $z < 0.4$. We used the DR12 CMASS galaxy catalogue and found 1 million pairs with similar selection criteria. Our sample is 5 times larger and covers a higher redshift range ($0.43 < z < 0.75$). These two catalogues are therefore independent and complementary in their redshift ranges. Despite the differences, we achieved similar results in terms of the amplitudes and statistical significances of the filament signal. In terms of the Compton y-parameter, T17 found $y \approx 1 \times 10^{-8}$ at the 5.3σ level, whereas we find $y \approx 0.6 \times 10^{-8}$ at the 5.1σ level. The fact that two independent studies using two different catalogues achieve similar conclusions provides strong evidence for the detection of gas filaments.

1. Persic, M. & Salucci, P. The baryon content of the universe. MNRAS **258**, 14P–18P (1992). astro-ph/0502178.

2. Fukugita, M. & Peebles, P. J. E. The Cosmic Energy Inventory. ApJ **616**, 643–668 (2004). astro-ph/0406095.

3. Planck Collaboration *et al.* Planck 2015 results. XIII. Cosmological parameters. A&A **594**,

A13 (2016). 1502.01589.

4. Cen, R. & Ostriker, J. P. Where Are the Baryons? ApJ **514**, 1–6 (1999). astro-ph/9806281.

5. Davé, R. *et al.* Baryons in the Warm-Hot Intergalactic Medium. ApJ **552**, 473–483 (2001). astro-ph/0007217.

6. Kull, A. & Böhringer, H. Detection of filamentary X-ray structure in the core of the Shapley supercluster. A&A **341**, 23–28 (1999). astro-ph/9812319.

7. Eckert, D., Jauzac, M., Shan, H. & et al. Warm-hot baryons comprise 5-10 per cent of filaments in the cosmic web. Nature **528**, 105–107 (2015). 1512.00454.

8. Penton, S. V., Stocke, J. T. & Shull, J. M. The Local Lyα Forest. IV. Space Telescope Imaging Spectrograph G140M Spectra and Results on the Distribution and Baryon Content of H I Absorbers. ApJS **152**, 29–62 (2004). astro-ph/0401036.

9. Shull, J. M., Smith, B. D. & Danforth, C. W. The Baryon Census in a Multiphase Intergalactic Medium: 30% of the Baryons May Still be Missing. ApJ **759**, 23 (2012). 1112.2706.

10. Sunyaev, R. A. & Zeldovich, Y. B. The Observations of Relic Radiation as a Test of the Nature of X-Ray Radiation from the Clusters of Galaxies. *Comments on Astrophysics and Space Physics* **4**, 173 (1972).

11. Planck Collaboration. 2015 results. XXII. A map of the thermal Sunyaev-Zeldovich effect. A&A **594**, A22 (2016). 1502.01596.

12. Colberg, J. M., Krughoff, K. S. & Connolly, A. J. Intercluster filaments in a ΛCDM Universe. MNRAS **359**, 272–282 (2005). astro-ph/0406665.

13. Alam, S. *et al.* The Eleventh and Twelfth Data Releases of the Sloan Digital Sky Survey: Final Data from SDSS-III. ApJS **219**, 12 (2015). 1501.00963.

14. Dawson, K. S. *et al.* The Baryon Oscillation Spectroscopic Survey of SDSS-III. AJ **145**, 10 (2013). 1208.0022.

15. Clampitt, J., Miyatake, H., Jain, B. & Takada, M. Detection of stacked filament lensing between SDSS luminous red galaxies. MNRAS **457**, 2391–2400 (2016). 1402.3302.

16. Epps, S. D. & Hudson, M. J. The Weak Lensing Masses of Filaments between Luminous Red Galaxies. MNRAS **468**, 2605–2613 (2017). 1702.08485.

17. Maraston, C. *et al.* Stellar masses of SDSS-III/BOSS galaxies at $z \sim 0.5$ and constraints to galaxy formation models. MNRAS **435**, 2764–2792 (2013). 1207.6114.

18. White, M. *et al.* The Clustering of Massive Galaxies at z ˜ 0.5 from the First Semester of BOSS Data. ApJ **728**, 126 (2011). 1010.4915.

19. Hurier, G., Macías-Pérez, J. F. & Hildebrandt, S. MILCA, a modified internal linear combination algorithm to extract astrophysical emissions from multifrequency sky maps. A&A **558**, A118 (2013). 1007.1149.

20. Górski, K. M. *et al.* HEALPix: A Framework for High-Resolution Discretization and Fast Analysis of Data Distributed on the Sphere. ApJ **622**, 759–771 (2005). astro-ph/0409513.

21. Greco, J. P., Hill, J. C., Spergel, D. N. & Battaglia, N. The Stacked Thermal Sunyaev-Zel'dovich Signal of Locally Brightest Galaxies in Planck Full Mission Data: Evidence for Galaxy Feedback? ApJ **808**, 151 (2015). 1409.6747.

22. Tanimura, H. *et al.* A Search for Warm/Hot Gas Filaments Between Pairs of SDSS Luminous Red Galaxies. *ArXiv e-prints* (2017). 1709.05024.

Acknowledgements We thank the Planck collaboration for making the full-sky y-map public.

We thank the SDSS collaboration for making public the CMASS galaxy catalogue. Funding for SDSS-III has been provided by the Alfred P. Sloan Foundation, the Participating Institutions, the National Science Foundation, and the U.S. Department of Energy Office of Science. The SDSS-III web site is http://www.sdss3.org/.

SDSS-III is managed by the Astrophysical Research Consortium for the Participating Institutions of the SDSS-III Collaboration including the University of Arizona, the Brazilian Participation Group, Brookhaven National Laboratory, Carnegie Mellon University, University of Florida, the French Participation Group, the German Participation Group, Harvard University, the Instituto de Astrofisica de Canarias, the Michigan State/Notre Dame/JINA Participation Group, Johns Hopkins University, Lawrence Berkeley National Laboratory, Max Planck Institute for Astrophysics, Max Planck Institute for Extraterrestrial Physics, New Mexico State University, New York University, Ohio State University, Pennsylvania State University, University of Portsmouth, Princeton University, the Spanish Participation Group, University of Tokyo, University of Utah, Vanderbilt University, University of Virginia, University of Washington, and Yale University.

AdG was supported by the Edinburgh School of Physics and Astronomy Career Development Summer Scholarship and the RSE Cormack Vacation Research Scholarship. YC, JAP and CH were supported by the European Research Council under grant numbers 670193 (YC; JAP) and 647112 (CH). We thank Martin White for useful discussions.

Author Contributions All authors contributed to the development and writing of this paper with YC conceiving the idea and methodology, AdG leading the data analysis, and AdG and YC co-writing the paper. This paper presents the findings of AdG's senior-honours undergraduate research project at the University of Edinburgh.

Competing Interests The authors declare that they have no competing financial interests.

Correspondence Correspondence and requests for materials should be addressed to YC (email: cai@roe.ac.uk).